Molecular Neurobiology (2019) 56:8277–8295
https://doi.org/10.1007/s12035-019-01645-2

Altered Gene Expression of Thyroid Hormone Transporters and Deiodinases in iPS MeCP2-Knockout Cells-Derived Neurons

Janaina Sena de Souza[1,2] · Divino Romão Ferreira[1] · Roberto Herai[3] · Cassiano Carromeu[2] · Laila Brito Torres[4,5] · Bruno Henrique Silva Araujo[6] · Fernanda Cugola[2] · Rui M. B. Maciel[1] · Alysson Renato Muotri[2] · Gisele Giannocco[1,7]

Received: 15 February 2019 / Accepted: 10 May 2019 / Published online: 18 June 2019

Abstract

MeCP2 is an X-linked gene; its mutation causes Rett Syndrome (RTT), a severe neurodevelopmental disability that affects mainly girls. Acting as a transcription factor, the MeCP2 protein is able to regulate several hormone-related genes, such as the thyroid hormones (TH), which are known to play an important role in the development of the central nervous system (CNS). Although only a few studies have associated RTT and TH, TH deficit can lead to neurological deregulation by triggering functional deficiencies during adulthood. Here, we used human-induced pluripotent stem cell (iPSC) to generate MeCP2-knockout neuronal progenitor cells and adult neurons. Using this cellular model, we then investigated the expression of genes associated with TH homeostasis, such as the TH transporters (*LAT1*, *LAT2*, *MCT8*, *MCT10*, and *OATP4A1*) and deiodinases (*DIO1*, *2*, and *3*). Then, we treated the neural cells with THs and analyzed the expression of several genes related to neurodevelopment and functional maintenance. Our results showed that several TH-related genes, such as deiodinases, are altered in RTT samples when compared to WT cells. Moreover, the treatment of the neural cells with THs increased the amount of MAP2 and synapsin-1 expression in RTT cells. Our work provided evidences that TH homeostasis is compromised in RTT-derived neural cells, which could be an important factor to contribute to the imbalance in the neurodevelopmental phenotype presented in this syndrome and can lead us to better understand other neurodevelopmental diseases.

Keywords *MeCP2* gene mutation · Rett syndrome · Thyroid hormones · Gene expression · Transporter · Deiodinase

Introduction

The mutations in the X-linked *MeCP2* gene cause Rett syndrome (RTT), a progressive neurological disorder that affects mainly girls [1, 2]. Acting as a chromatin remodeler, the coded MeCP2 protein is involved in the epigenetic control of gene regulation, by binding to CpG dinucleotide of gene promoters, suppressing or inducing transcription [3, 4]. Several mutations in this gene have been associated with RTT cellular phenotypes, such as decreased number of synapses, reduced soma

Electronic supplementary material The online version of this article (https://doi.org/10.1007/s12035-019-01645-2) contains supplementary material, which is available to authorized users.

✉ Janaina Sena de Souza
ninasenasouza@gmail.com

[1] Departamento de Medicina, Laboratório de Endocrinologia e Medicina Translacional, Universidade Federal de São Paulo, UNIFESP/EPM, Rua Pedro de Toledo, 669 – 11 andar, São Paulo, SP 04039-032, Brazil

[2] Department of Pediatrics, School of Medicine, University of California, San Diego, La Jolla, CA 92093, USA

[3] Graduate Program in Health Sciences, School of Medicine, Pontifícia Universidade Católica do Paraná (PUCPR/PPGCS), Curitiba, PR 80215-901, Brazil

[4] Faculdade São Leopoldo Mandic, Área de Fisiologia, Farmacologia, Instituto São Leopoldo Mandic, Campinas, Brazil

[5] Department of Genetics and Evolutionary Biology, Human Genome and Stem Cell Research Center, Institute of Biociences, Universidade de São Paulo (USP), São Paulo, Brazil

[6] Brazilian Biosciences National Laboratory (LNBio), Brazilian Center for Research in Energy and Materials (CNPEM), Campinas, SP Zip Code 13083-970, Brazil

[7] Departamento de Ciências Biológicas, Universidade Federal de São Paulo, UNIFESP, Diadema, SP 09920-000, Brazil

size, and aberrant neuronal dendritic maturation [4]. More recently, our group showed that *MeCP2* mutation can also affect the expression of TH receptors in RTT syndrome and that IGF1 treatment, a candidate drug for RTT syndrome, may be dependent of thyroid hormone receptor alpha 3 (*THRA3*) expression [5]. However, there is still missing a complete understanding of the role of thyroid hormones (THs) in RTT.

Children suffering from severe hypothyroidism condition, caused by TH production alterations, if not treated, can develop an intellectual disability, deaf-mutism, spastic dysplasia, and extrapyramidal stiffness [6–12]. The main cause of THs deficiency is the lack of adequate iodine intake during pregnancy, which may affect their synthesis and may cause neurological symptoms, such as neurological cretinism [13, 14]. It was also shown that even a slight decrease of thyroxin production during pregnancy increases the risk of abnormal neuronal development and may lead to a decrease in the progeny intellectual quotient [11, 15, 16]. Furthermore, TH deficiency during critical stages of brain development, such as fetal and neonatal periods, are also associated with a reduced number of cells, affected synaptogenesis and dendritic branching, as well as decreased cell migration and axon myelination [17].

The fine tune control of these hormones is essential for normal brain development. Our hypothesis is that RTT patients may have a dysfunction in TH hormone maintenance and that alteration may be, at least in part, related to the neurological developmental impairment in RTT individuals. And as expected, we showed that TH-related gene expression is altered in RTT, suggesting that these hormones can play an important role in RTT clinical phenotype.

These findings, connecting TH alterations with neurological pathogenesis, are explained by the fact that the brain is the major target organ of TH (pro-hormone thyroxin, T4 and its active metabolite 3, 5, 3′-triiodothyronine, T3). When TH expression is altered during brain maturation, it can cause negative effects in the nervous system developmental processes, by directly acting in several cellular processes of neurons and glial cells, affecting differentiation, myelination, cytoskeleton stabilization, and cell signaling [18–20].

The main type of TH is T4, a pro-hormone that is produced and secreted by the thyroid gland (80%), having their receptors more affinity for T3. Within target tissues, T4 is converted into T3 by deiodinases in order to be activated. T4 is the form of TH that is believed to cross the blood-brain barrier (BBB) in the adult brain [21].

When TH levels are low, deiodinase type 2 (DIO2) expression increases in the brain, but at elevated levels, TH could increase deiodinase type 3 (DIO3) enzyme activity. These enzymes protect the brain from the damaging effect of hypo- and hyperthyroidism. However, unlike other tissues (liver and kidney, for example), the brain requires more time to balance TH at the right concentration, suggesting that abrupt changes of TH could cause severe damages in the brain [21].

Generally, T3 and T4 hormones are transported to the brain by TH-specific transporters [22, 23]. These transporters are divided into three main families: organic anion-transporting polypeptides (OATP), L-type amino acid transporter (LAT), and the monocarboxylate transporter (MCT) [11, 24, 25].

T3 interacts with receptors located into specific *loci* of genomic DNA, known as thyroid hormone responsive elements (TREs). The interaction between the complex TH/nuclear receptor with the TREs leads to transcription activation or inhibition of genes associated with TH [5, 26–28]. Additionally, TH receptors also have activity in the no bonded hormone state. This type of regulation is still unclear but preliminary data has shown they may have a role in the genesis of the hypothyroidism phenotype [21, 29].

Therefore, few studies explore the role of TH alteration and neurological impairment in RTT individuals. Here, we investigated the gene expression of proteins related to TH regulation in neurons derived from iPSC of RTT patient. Our results showed that TH-related gene expression is altered in RTT, suggesting that TH alteration can play an important role in RTT clinical phenotype.

Material and Methods

Ethics Committee

This study is part of a reviewed and approved research by the UCSD Human Research Protections Program and it is in accordance with requirements of the Code of Federal Regulations on the Protection of Human Subjects (reference number is 090801ZF). After a complete description of the study, written informed consent was signed.

Cell Culture

Induced Pluripotent Stem Cells

iPSCs from our laboratory cell library were used in this study. iPSC derived from a male patient with RTT, with a nonsense mutation at position 83 of the protein (RTT), and healthy male control cells (WT) were used. iPSC clones were propagated clonally (3–4 clones) on feeders, using mTeSR medium (*StemCell Technologies*, Tukwila, WA, EUA). Cytogenetic analysis was performed in all clones to evaluate correct cell karyotype at the Children's Hospital in Los Angeles.

Generation of Embryonic Bodies and Neural Rosettes

To generate embryonic bodies (EBs), iPSCs were treated for 2 days in N2 medium (DMEM/F-12 50/50, with L-glutamine and 15 mM HEPES; insulin; progesterone, sodium selenite, L-glutamine, HEPES, Apo-transferrin) with 1 μM Dorsomorphin

(DM) and 10 μM SB431542 (Stemgent, Cambridge, MA, EUA). After that, the cells were maintained in suspension for approximately 1 week with N2 medium [5, 30]. After 5–7 days, EBs were collected and seeded in 6-cm coated matrigel plate. After approximately 7 days, the rosettes were manually collected, dissociated to single cells, and maintained in NGF medium (DMEM/F-12 supplemented with 0.5× N2, 0.5× Gem21, 1% penicillin/streptomycin, and 20 ng/mL of bFGF). The obtained Neural Progenitor Cells (NPCs) were plated on poly-ornithine (10 μg/mL, Sigma-Aldrich) and laminin (2.5 μg/mL, Gibco)-coated plates and cultured with NGF medium.

NPCs Expansion and Neural Cell (NE) Differentiation

NPCs were propagated until the fifth passage in a density of 10^6 cells. After this, they were seeded into six-well plates in a density of 7×10^5 cells per well. Then, the differentiation into neurons was induced with NG medium (DMEM/F-12 supplemented with 0.5× N2, 0.5× Gem21, and 1× penicillin/streptomycin) supplemented with 10 μM ROCK Inhibitor (Ri) (Tocris Bioscience) for 48 h, and then the cells were kept in NG medium without Ri up to 6 weeks for neural maturation.

Cell Treatment

Six-week neural cells were treated with THs for 48 h before being collected. Wild-type cells (WT) and Rett Syndrome cells (RTT) and the neuronal cells were treated as follows, control (CRTL), cells that had the media changed by a new volume of NG medium; T3.1, cells treated with NG medium complemented with a dose of 10^{-6} M of T3 (triiodothyronine); T3.2, cells treated with NG medium complemented with a dose of 10^{-12} M of T3; T4, cells treated with NG medium complemented with a dose of 20 pM of T4 (iodothyronine); and rT3, cell treated with NG medium complemented with a dose of 20 nM of rT3 (reverse T3). After treatment, these cells were collected for mRNA, in cell western and immunofluorescence analyzes [31].

RNA Extraction and qRT-PCR

Total RNA was extracted using TRIzol™ Reagent (Life Technologies). cDNA was synthesized by taking 1 μg of total RNA and QuantiTec Reverse Transcription Kit (Qiagen) was used as the manufacturer's instruction. Quantitative reverse-transcriptase PCR (qRT-PCR) was performed using gene-specific primers and QuantiTect SYBR Green PCR Kit (Qiagen). Quantification was made at *ABI Prism 5700 detector* (Applied Biosystems). The expression of target genes (Supplementary Table S1 and S2) and the endogenous control (GAPDH) were measured with technical duplicates in each qRT-PCR reaction. To obtain statistical significance, values from a minimum of three independent differentiation qRT-PCR runs were considered. The cycle threshold number (Ct) was calculated automatically by the program (Life Technologies, USA). The relative expressions of each target gene across differentiation days were normalized using the $2^{(\Delta\Delta Ct)}$ method compared with control [32].

Immunocytochemistry

Cells were fixed with 4% paraformaldehyde (PFA) for 20 min at room temperature (RT). Then, permeabilized and blocked using a SuperBlock™ (Thermo Scientific) blocking buffer for 30 min at RT. Primary antibodies were incubated overnight at 4 °C. Secondary antibodies were incubated for 1 h at RT. Cells were washed three times with phosphate-buffered saline (PBS) + 0.1% Tween-20. DAPI (Dako) was used to visualize nuclei. Coverslips were mounted on slides using Prolong Gold mounting medium (Life Technologies). Images were acquired using confocal microscope Radiance 2100 (Zeiss, Oberkochen, Germany) equipped with an upright microscope (Eclipse E800; Nikon, Tokyo, Japan). The pictures of each treated group were analyzed in ImageJ for MAP2 (1:1000) and synapsin-1 (1:250) quantification.

Hormonal Dosage

After 48 h of cell treatment with THs (control, T3 10^{-6} and 10^{-12} M, T4 20 pM, and rT3 20 nM), the medium was collected and frozen until hormonal dosage. Thyroid hormones concentration was determined by electrochemiluminescence immunoassay method (Elecsys® Systems Roche Diagnostic Kit) following the recommendations of the manufacturer's protocol.

Genetic Network and Protein-Protein Interaction Network Analysis

TH-related genes were subjected to genetic interaction network-based analysis using the Pathway Commons software [33]. To create the network, the software was configured using the following parameters: input molecule = MeCP2, query type = neighborhood, number of genes = 29, and interaction types = control expression.

Additionally, we also performed a protein-protein interaction analysis by subjecting the corresponding proteins of TH-related genes to the String Protein Interaction software [34]. To create the interaction network, the software was configured using the following parameters: active interaction sources (set to textmining, experiments, and database); minimum required interaction score (set to 0.400); and max number of interactors to show (set to 20 at first shell, and 40 as the second shell).

Statistical Analysis

Results were first submitted to the Shapiro-Wilk normality test. The parameters were analyzed by one-way ANOVA followed

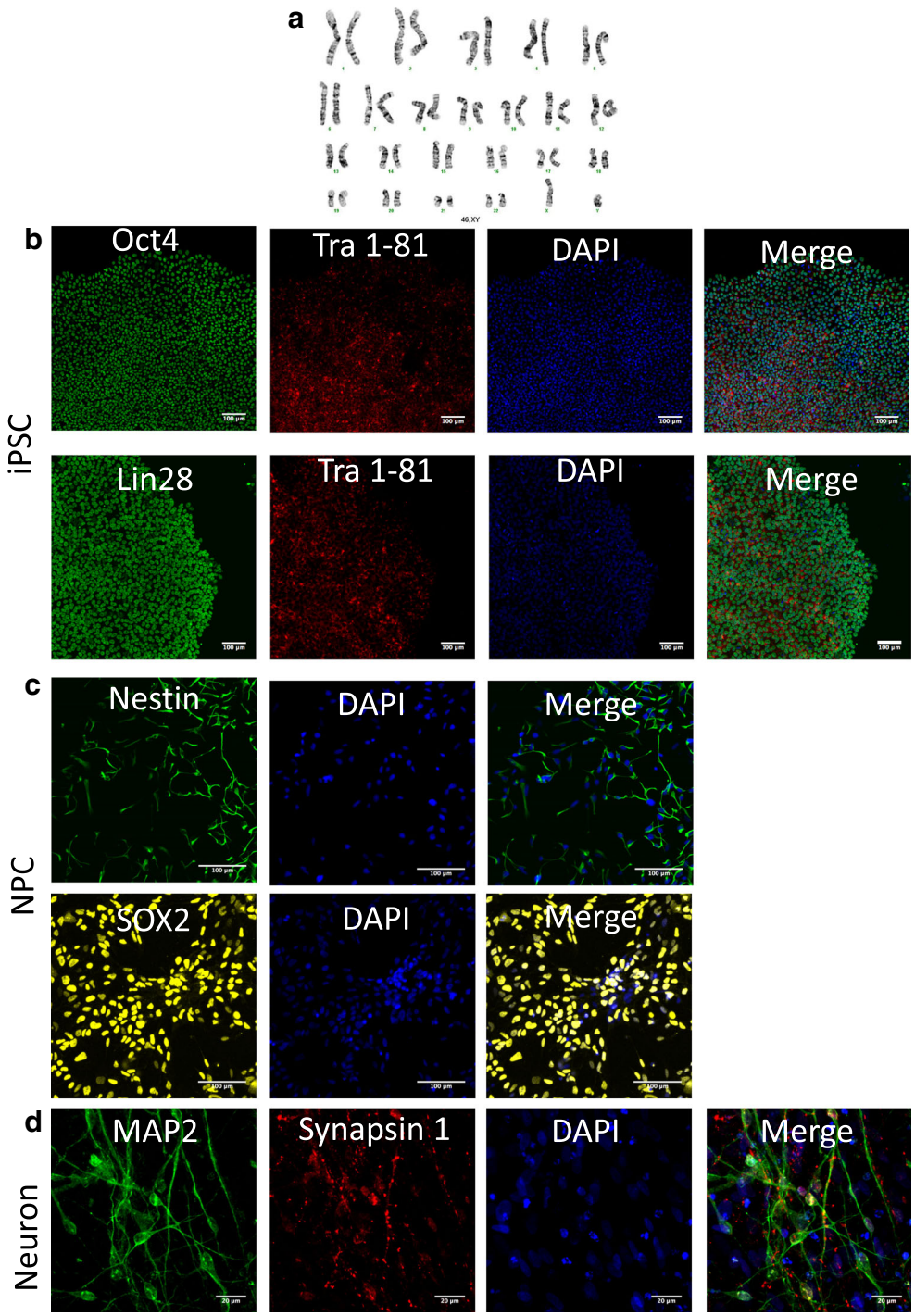

Fig. 1 Cell karyotyping and immunofluorescence cell characterization. The male cells analyzed in this study presented chromosome number that matches with normal karyotyping. They also showed expression of specific protein markers associated to each cell stage—iPSC, NPC, and neurons. **a** This image shows the representative cell karyotyping at neural progenitor cell stage and displays that the studied cells are from male WT and affected individuals and present normal chromosome number (46, XY). Banding method (resolution), G-Banding; number of cells counted, 20; number of cells karyotyped, 5. **b** Images of induced Pluripotent Stem Cells (iPSC) presenting expression of specific protein markers for this type of cell after approximately 5–6 days of colony passage. Top: Oct4 (green), Tra 1-81 (red), DAPI (blue), and Merge. Bottom: Lin28 (green), Tra 1-81 (red), DAPI (blue), and Merge. Scale bar = 100 μm. Immunofluorescence images. **c** Neural Progenitor Cells (NPC) show expression of specific protein markers for this type of cell after confluence of approximately 50%. Top: Nestin (green), DAPI (blue), and Merge. Bottom: SOX2 (yellow), DAPI (blue), and Merge. Scale bar = 100 μm. Immunofluorescence images. **d** Neurons show the expression of specific protein markers for this type of cell after 6 weeks of induced differentiation. MAP2 (green), synapsin-1 (red), DAPI (blue), and Merge. Scale bar = 20 μm. Immunofluorescence images

by Newman-Keuls Multiple Comparison test, and Kruskal-Wallis, followed by Dunn's multiple comparison test. Pearson correlation analysis was performed to evaluate the relationship strength between variables obtained from the same sample. The *r* values rage from + 1 to − 1, where + 1 is an exact correlation and − 1 is an exact inverse correlation. All analyses were performed with *GraphPad Prism* (La Jolla, CA, USA). Statistical differences were considered significant when the *p* value was lower than 0.05. The values were expressed as means and the standard error of the mean (± SEM).

Results

Characterization

Karyotyping test showed normal chromosomal organization considering size and number of somatic and non-somatic chromosomes. (Fig. 1a).

Canonical marker analyses were carried out on iPSC (induced Pluripotent Stem Cell), NPC (neural progenitor cell) and NE (neural cell) cells. For iPSC, the considered protein markers were OCT4, TRA181, and LIN28 (Fig. 1b). At the NPC stage, we used the antibodies targeting the SOX2 and NESTIN proteins, both markers of neural stem cells (Fig. 1c). For neurons, we used the specific neuronal markers MAP2 and synapsin-1 (Fig. 1d).

Hormone Dosage after Cell Treatment

For hormone dosage analysis (Table 1), we collected media after 48 h treatment of 6-week cultured neural cells. Our results showed an increased T3 concentration in T3 10^{-6} M (> 10.00 nmol/L) treated group compared to the samples controls (1.35 ± 0.05 nmol/L), T3 10^{-12} M (1.34 ± 0.04 nmol/L), and rT3 (1.31 ± 0.03 nmol/L). Similarly, we also found in the T4-treated group (5.11 ± 0.31 nmol/L) an increased concentration of T3 compared to control, T3 10^{-12} M and rT3.

T4 concentration was increased in the group treated with T4 (> 320.00 nmol/L) compared to the samples control (9.61 ± 0.06 nmol/L), T3 10^{-12} M, and rT3 (9.67 ± 0.07 nmol/L). The T3 10^{-6} M (11.18 ± 0.42 nmol/L)-treated group presented T4 concentration as increased compared to control and rT3 groups.

Thyroid Hormone Transporters Have Altered Gene Expression in RTT

Based on our quantification analysis, we demonstrated that RTT cells have altered the expression of important TH-related gene transporters during developmental stages (iPSC-induced pluripotent stem cells, EB-embryoid stem cells, NPC-neuronal progenitor cells, NE-neuron cells) when compared to the relative WT samples.

Table 1 Media level of T3 and T4 in the control, T3 10^{-6} M, T3 10^{-12} M, rT3 (20 nM), and T4 (20 pM) treated groups. The significance among the groups was determined by one-way ANOVA followed by Newman-Keuls posttest

Groups	T3 (nmol/L)	T4 (nmol/L)
Control	1.347 ± 0.054	9.608 ± 0.057
T3 10^{-6} M	> 10.000***	11.180 ± 0.423**
T3 10^{-12} M	1.342 ± 0.038	9.791 ± 0.083
rT3	1.306 ± 0.026	9.667 ± 0.071*
T4	5.106 ± 0.3136*	> 320.0***

T3: ***$P < 0.0001$ T3 10^{-6} M vs. Control, T3 10^{-12} M, rT3; *$P < 0.05$ T4 vs. Control, T3 10^{-12} M and rT3. T4: ***$P < 0.0001$ T4 vs. Control, T3 10^{-12} M, rT3; **$P < 0.001$ vs. Control, *$P < 0.05$ vs. T3 10^{-6} M. Values are the mean ± SEM ($n = 12$)

MCT8 gene expression was altered in three cell stages. In the EB stage (Fig. 2c), it was increased 2.1-fold in RTT (2.12 ± 0.40) compared to WT (1.02 ± 0.10). In the NPC stage (Fig. 2e), it was decreased 0.3-fold in RTT (0.77 ± 0.03) compared to WT (1.03 ± 0.10). In neural cells (Fig. 2i), we found *MCT8* expression was increased 1.9-fold in RTT (2.12 ± 0.23) compared to WT (1.12 ± 0.26).

MCT10 gene expression was altered in three studied stages. In the iPSC stage (Fig. 2a), the gene expression was decreased in RTT (0.77 ± 0.06) 0.3 times compared to WT (1.01 ± 0.08). In the NPCs (Fig. 2f), the expression of *MCT10* was increased by 2-fold in RTT (2.35 ± 0.19) compared to WT (1.17 ± 0.28). It was also increased by 2.1-fold in RTT (2.36 ± 0.22) compared to WT (1.13 ± 0.27) at neural cells (Fig. 2j).

In RTT NPC cells (Fig. 2g), we found that *LAT1* expression was significantly decreased by 2.7-fold in RTT (0.43 ± 0.08) compared to WT (1.17 ± 0.28).

Gene expression of *LAT2* was 0.8-fold significant increased in RTT (1.27 ± 0.10) compared to WT (1.01 ± 0.05) in iPSC stage (Fig. 2b).

At the EB stage, *OATP4A1* expression was increased 2.6-fold in RTT (2.61 ± 0.72) compared to WT (1.02 ± 0.10) (Fig. 2d).

Thyroid Hormone Delivery May Be Impaired in Rett Syndrome Due to Altered Deiodinases

Another family of TH-related molecules investigated was the deiodinases, a class of enzymes responsible for the control of thyroid hormone status within the cells.

We found that in EBs stage (Fig. 3b) *DIO1* expression was 1.9-fold increased in RTT (1.89 ± 0.33) compared to WT (1.00 ± 0.03). In NPC (Fig. 3d), *DIO1* expression was 2-fold increased in RTT (2.12 ± 0.19) compared to WT (1.05 ± 0.14).

In addition, *DIO2* was increased 1.6-fold in RTT cells (1.72 ± 0.15) compared to WT (1.05 ± 0.15) during

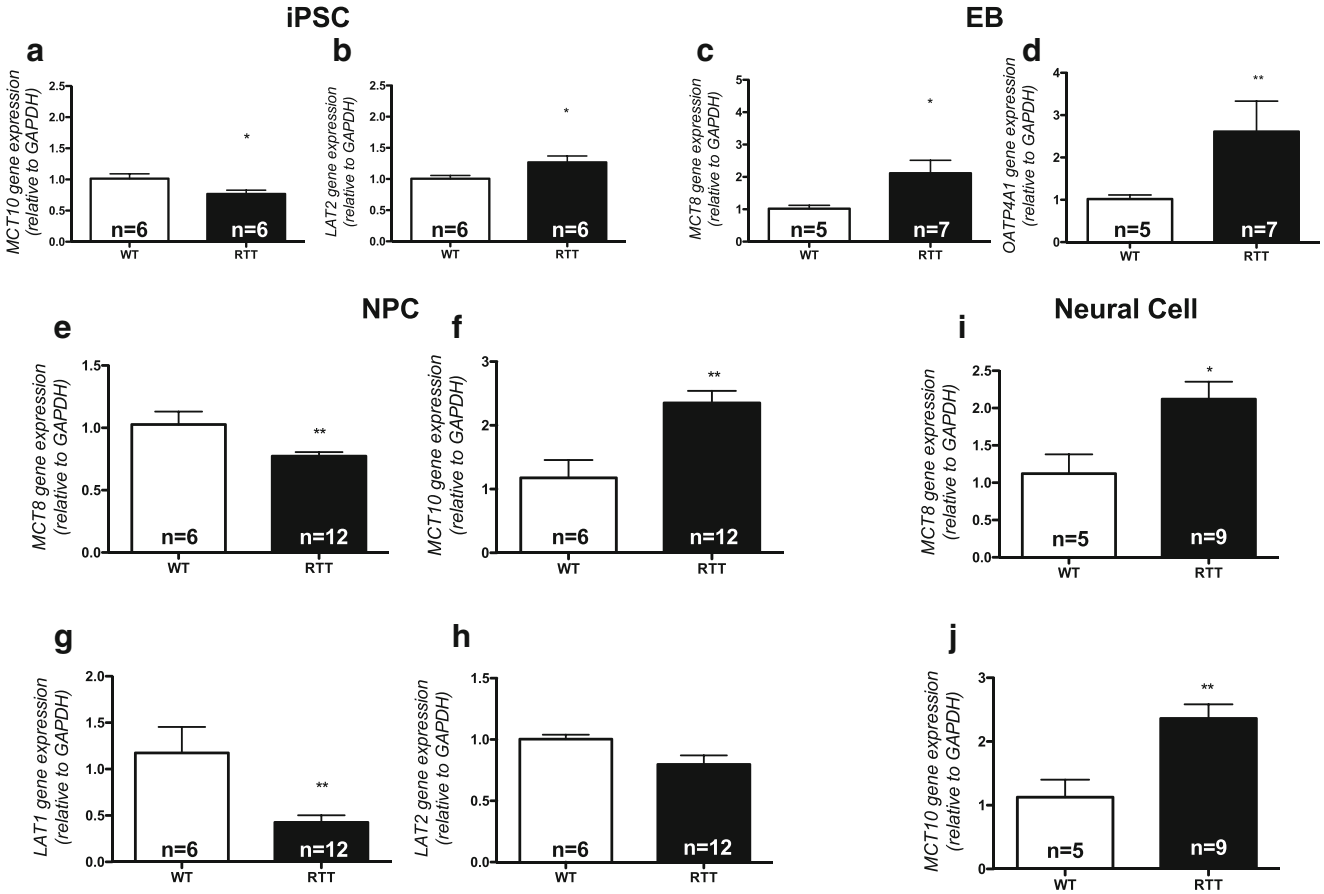

Fig. 2 TH Transporters in RTT are altered. **a**–**b** Graphic representation of gene expression of thyroid hormone transporters in iPSC stage comparing WT and RTT cells. *$P < 0.05$ vs. WT. **c**–**d** Graphic representation of gene expression of thyroid hormone transporters in EB stage comparing WT and RTT cells. **$P < 0.01$ vs. WT; *$P < 0.05$ vs. WT. **e**–**h** Graphic representation of gene expression of thyroid hormone transporters in NPC stage comparing WT and RTT cells. **$P < 0.01$ vs. WT. **a**–**b** Graphic representation of gene expression of thyroid hormone transporters in Neural Cell stage comparing WT and RTT cells. **$P < 0.01$ vs. WT; *$P < 0.05$ vs. WT. Values are the mean ± SEM

the iPSC stage (Fig. 3a). We also observed a decreased expression of 7-fold in neural cells stage (Fig. 3f) at RTT cells (0.17 ± 0.02) when compared to WT (1.19 ± 0.34).

We also evaluated the expression of *DIO3*. Our results showed that at EBs stage (Fig. 3c), *DIO3* is 4.9-fold increased in RTT (5.24 ± 2.12) compared to WT (1.06 ± 0.18) and, at NPC stage (Fig. 3e), it was 12.5-fold increased in RTT (11.29 ± 2.55) compared to WT (1.21 ± 0.31).

Neural Cells Treated with THs Had DIO3 and NTF3 Expression Altered

Six-week neural cells were kept in media with THs for 48 h; after this period, they were collected and the mRNA was analyzed. Among many genes studied, *DIO3* expression increased in RTT cells (Fig. 4b) treated with T3 10^{-6} M (1.96 ± 0.29) 1.9-fold and rT3 (1.78 ± 0.26) 1.8-fold compared to CTRL (1.01 ± 0.10). *NTF3* gene expression increased in WT cells (Fig. 4c) at the group treated with T3 10^{-6} M (1.31 ± 0.31) 2-fold compared to the control group (0.66 ± 0.87).

Increased Expression of Neuropilin 2 in RTT

Neuropilin 2 is a receptor of semaphorins, guidance proteins that are altered in neurodevelopmental diseases, such as autism [35]; in our study, it was increased 1.9-fold in RTT cells (1.52 ± 0.24) compared to WT cells (0.81 ± 0.16) (Fig. 4e).

Thyroid Hormone Regulates Synapsin-1 and MAP2 Content in Human iPSC-Derived Neural Cells

Six-week neural cells were treated with thyroid hormones (T3, 10^{-6} M and 10^{-12} M; T4, 20 pM; and rT3, 20 nM) for 48 h and then analyzed for synapsin-1 and MAP2 content.

Non-affected cells (WT) treated with T4 (1367 ± 0.099) increased 36% the amount of synapsin-1 compared to WT control (1005 ± 0.105) (Fig. 5a). On the other hand, the amount of MAP2 did not increase in the treated groups compared with control.

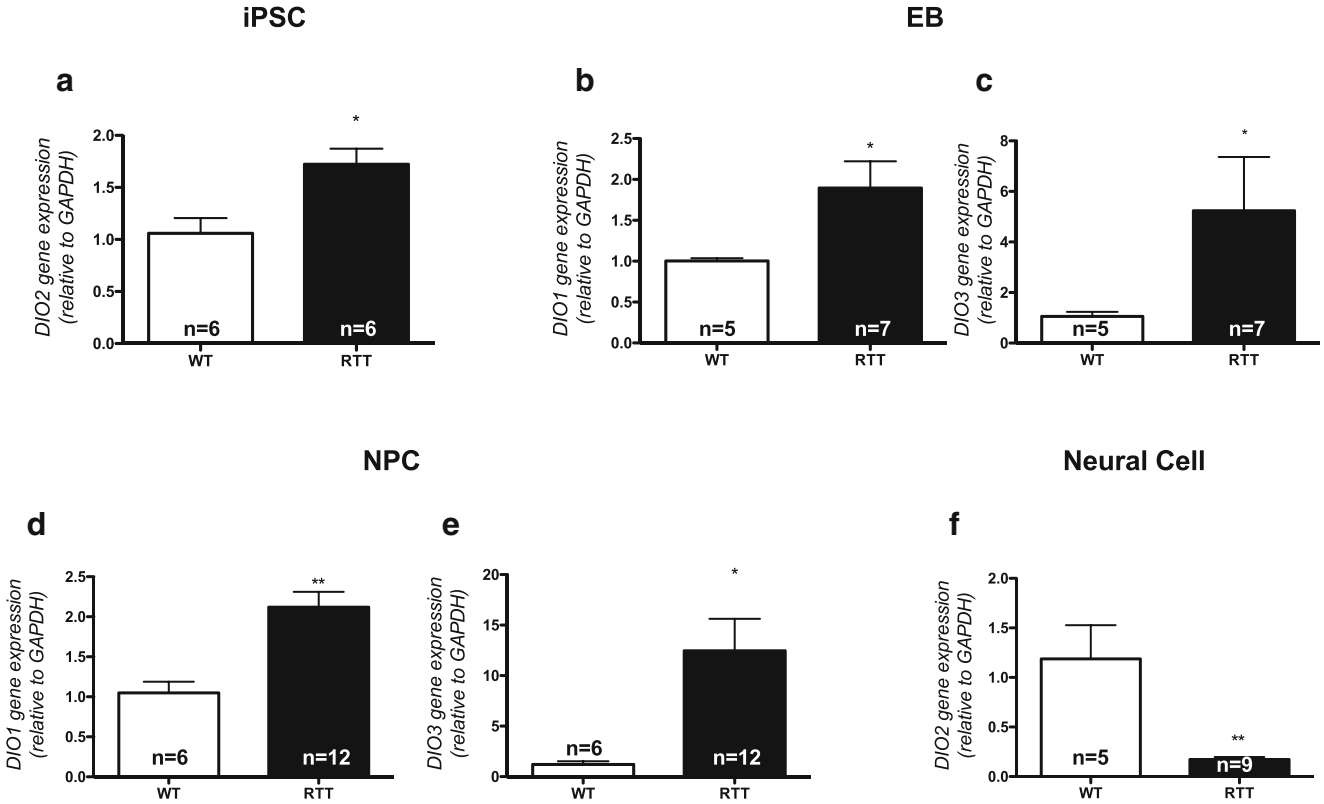

Fig. 3 Deiodinases, important enzymes for the maintenance of thyroid hormone status in the target tissue and that are already associated with mental disability, are altered in the studied cells. **a** Graphic representation of gene expression of deiodinases type 2 in iPSC stage comparing WT and RTT cells. $*P < 0.05$ vs. WT. **b**–**c** Graphic representation of gene expression of deiodinases type 1 and type 3 in EB stage comparing WT and RTT cells. $*P < 0.05$ vs. WT. **d**–**e** Graphic representation of gene expression of deiodinases type 1 and type 3 in NPC stage comparing WT and RTT cells. $**P < 0.01$ vs. WT; $*P < 0.05$ vs. WT. **f** Graphic representation of gene expression of deiodinases type 2 in Neural Cell stage comparing WT and RTT cells. $**P < 0.01$ vs. WT. Values are the mean ± SEM

In RTT neurons, the content of synapsin-1 and MAP2 were decreased compared to WT cells. When these 6-week neural cells were treated with THs, the amount of both proteins increased in the cells treated with 10^{-12} M of T3 and rT3. Synapsin-1 content was increased 25% in 10^{-12} M-treated cells (0.591 ± 0.018) and 27% in rT3-treated cells (0.602 ± 0.034), when compared to control. MAP2 increased 54% in the 10^{-12} M group (0.337 ± 0.023) and increased 43% in the rT3 group (0.314 ± 0.018), compared to control.

Altered TH-Related Genes in RTT Can Affect Cellular Metabolic Pathways

We performed genetic interaction analysis of those TH-related genes that showed significant gene expression modification in neuronal cells derived from iPSC-RTT patients. The expression of these genes, four in total (*DIO2*, *SLC16A2/MCT8*, *SLC16A10/MCT10*, and *NRP2*), might interfere with the expression of each other since they all can indirectly interact (Fig. 6). The gene *DIO2* interacts with *NRP2* through four distinct genes: *TCF3*, *LEF1*, *ZEB1*, and *LMO2*. *NRP2* can interact with *SLC16A2* through three distinct genes: *TFDP1*, *FOXO4*, and *CYP26A1*. *SLC16A2* can interact with *SLC16A10* trough the *PAX4* gene. These same four genes were also subjected to protein-protein interaction network analysis, and also showed to indirectly connect with each other (Fig. 7).

Another important analysis we performed was to show possible genetic connections of *MeCP2* (Fig. 8). According to the network, this gene could interact and regulate several other types of genes, such as the *GATA3*, which was previously correlated with neurological disorders [36].

Correlation Analysis of Investigated Genes

There are many correlation of gene expression (Table 2) presented in the Pearson's correlation of genes studied at the neural cell stage; however, herein, we outlined only the correlations higher than 0.850. *DIO1* has a high correlation with *NPR1* ($r = 0.860$) and *SEMA3A* ($r = 0.863$). *DIO3* has high correlation with *BDNF* ($r = 0.928$), *MAP2* ($r = 0.927$), *NRX1* ($r = 0.853$), and *SEMA3A* ($r = 0.889$). *MCT8* has high correlation with *MCT10* ($r = 0.959$) and *NLGN4* ($r = 0.854$). *BDNF* has high correlation with *MAP2* ($r = 0.933$), *NRX1* ($r = 0.863$),

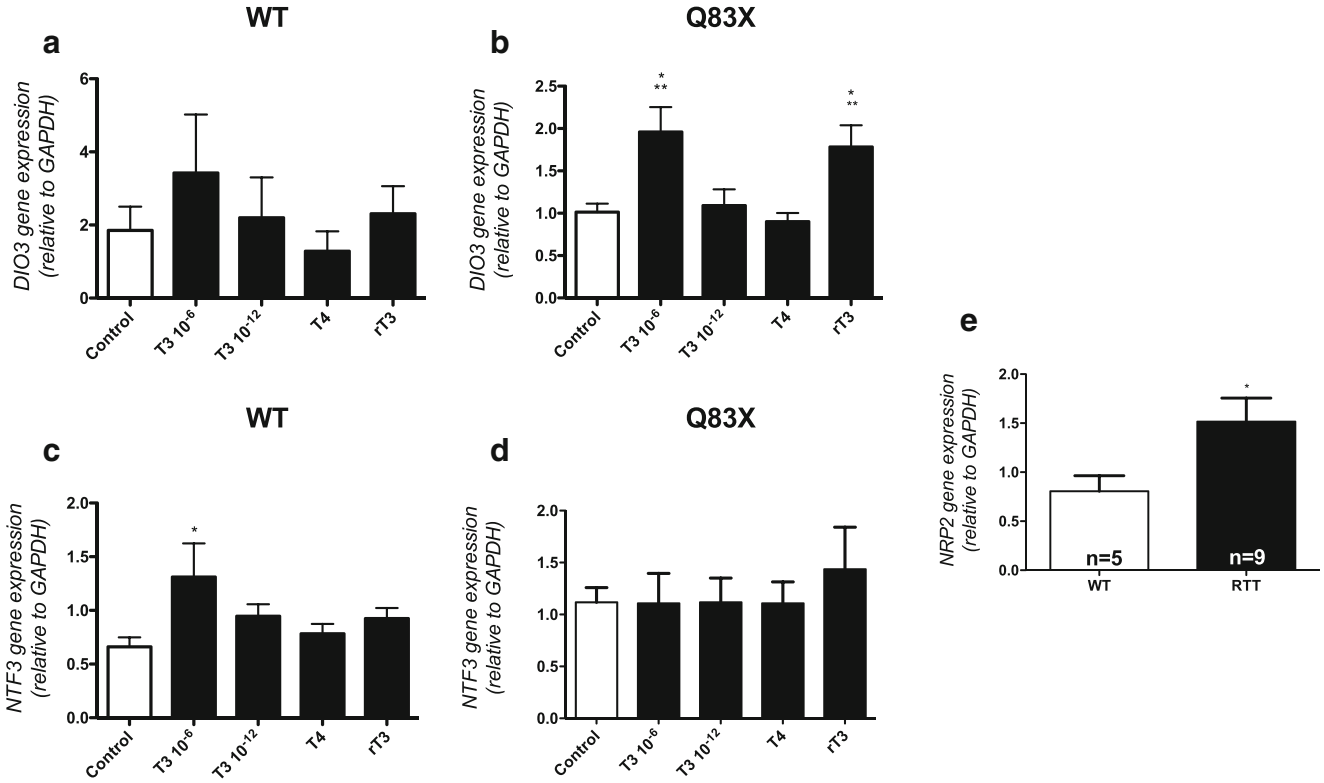

Fig. 4 Neural cell treatment with thyroid hormones changed gene expression of DIO3 in RTT cells and of NTF3 in WT cells. NRP2, an axonal guidance protein, is increased in RTT neural cells. **a**–**d** Graphic representation of DIO3 a–b and NTF3 c–d gene expression in WT and RTT neural cells treated with THs (T3, 10^{-6} M and 10^{-12} M; T4, 20 pM; and rT3, 20 nM) for 48 h after differentiation for 6 weeks (treated neural cells WT $n = 5$, Q83X $n = 9$). $^{*}P < 0.05$ vs. control; $^{**}P < 0.001$ vs. control. **e** Gene expression of NPR2 in 6 weeks differentiated neural cells of WT and RTT cells. In RTT cells, the expression of NRP2 is increased compared to WT. $^{*}P < 0.05$ vs. WT. Values are the mean ± SEM

and *PLXNA1* ($r = 0.858$). *CYTG* has strong correlation with *NaKATPase* ($r = 0.983$), *NCAM* ($r = 0.986$), *NGF* ($r = 0.977$), and *SYT1* ($r = 0.967$). *MAP2* has strong correlation with *NLGN3* ($r = 0.882$) and *NRX1* ($r = 0.966$). *NaKATPase* has strong correlation with *NCAM* ($r = 0{,}996$), *NGB* ($r = 0.874$), *NGF* ($r = 0.982$), and *SYT1* ($r = 0.991$). *NCAM* has strong correlation with *NGB* ($r = 0.890$), *NGF* ($r = 0.971$), and *SYT1* ($r = 0.995$). *NPR1* has strong correlation with *NPR2* ($r = 0.850$) and *SEMA3C* ($r = 0.881$). *NPR2* has high correlation with *PLXNA1* ($r = 0.937$), *SEMA5A* ($r = 0.900$), and *SHANK3* ($r = 0.851$). *SYT1* has high correlation with *NGB* ($r = 0.921$) and *NGF* ($r = 0.954$). *NLGN3* has high correlation with *NRX1* ($r = 0.930$) and *SYN1* ($r = 0.882$). *NLGN4* has high correlation with *NRX1* ($r = 0.883$). *SHANK3* has strong correlation with *PLXNA1* ($r = 0.913$) and *SYN1* ($r = 0.882$).

Discussion

Thyroid hormones play a critical role in the physiology and development of the organism, and can regulate a number of pathways involved in the development and maintenance of the fetal, postnatal, and adult central nervous system (CNS). Indeed, the importance of TH in development is perhaps most apparent in the CNS, where several TH deficiencies have been detected during the fetal and neonatal periods, leading to cretinism [21, 23, 37].

Only a few studies have shown a correlation between RTT and TH status. For example, Stagi et al. [2] showed that FT4 levels were higher in RTT patients, when compared to controls [2]. Therefore, the present study provides further evidence for the involvement of TH homeostasis neuronal cell development in RTT brains.

It is known that TH is essential for the development of several tissues, and that the brain is an important target [12]. Despite several studies showing the effect of TH on neuronal cell development, there are few examples in the literature investigating TH homeostasis in the RTT brain, or the reprogrammed cells derived from this syndrome. More recently, in 2017, de Souza et al. [5] showed that TH receptors gene expression is altered in RTT and that these receptors may be associated with IGF1 action. As an extension to this observation, the present study sought to compare the gene expression levels of TH transporters and deiodinases in RTT and control cells.

TH traverses the blood-brain barrier (BBB), via specific transporters. Due to the high affinity of T4 for these transporters (i.e., MCT8), it is believed that greater quantities of

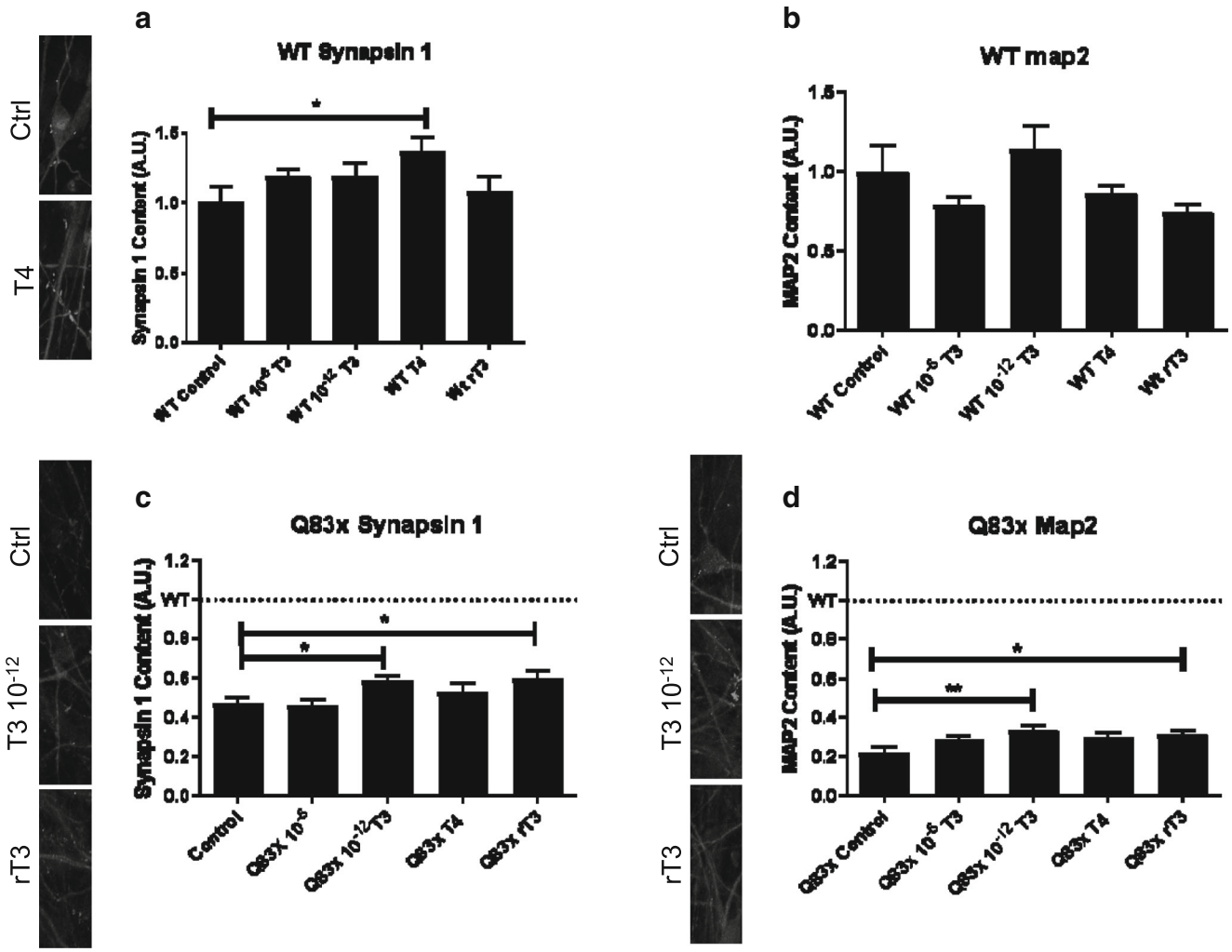

Fig. 5 Thyroid hormones increase synapsin-1 and MAP2 protein content in 6-week WT and RTT neural cells. **a** Synapsin-1 in WT neural cells after treatment with THs (T3, 10^{-6} M and 10^{-12} M; T4, 20 pM; and rT3, 20 nM) for 48 h. Synapsin-1 content increased in 6 weeks control (non-affected) neural cells after treatment with T4. $^{*}P < 0.05$ WT T4 vs. WT control. In the left of **a,** the pictures represent the graphic results; in red synapsin-1, in green MAP2. **b** MAP2 in WT neuronal cells after treatment with THs (T3, 10^{-6} M and 10^{-12} M; T4, 20 pM; and rT3, 20 nM) for 48 h. MAP2 content did not change in 6 weeks control (non-affected) neural cells. **c** Synapsin-1 in RTT neural cells after treatment with THs (T3, 10^{-6} M and 10^{-12} M; T4, 20 pM; and rT3, 20 nM) for 48 h. Synapsin-1 content increased in 6 weeks control (RTT) neural cells after treatment with 10^{-12} T3 and rT3. $^{*}P < 0.05$ Q83X 10^{-12} T3 and rT3 vs. Q83X control. The content of synapsin-1 is decreased in Q83X neural cells compared to WT cells. In the left of **c**, the pictures represent the graphic results; in red synapsin-1, in green MAP2. **d** MAP2 in RTT neural cells after treatment with THs (T3, 10^{-6} M and 10^{-12} M; T4, 20 pM; and rT3, 20 nM) for 48 h. MAP2 content increased in 6 weeks control (RTT) neural cells after treatment with 10^{-12} T3 and rT3. $^{**}P < 0.01$ Q83X 10^{-12} T3 vs. control; $^{*}P < 0.05$ rT3 vs. Q83X control. The content of MAP2 is decreased in Q83X neural cells compared to WT cells. In the left of **d**, the pictures represent the graphic results; in red synapsin-1, in green MAP2

T4 enter the brain, when compared to the T3. T4 is then transported to astrocytes, through OATP, and activated into T3 by DIO2; T3 is then transported to the neurons by MCT8 [21]. Our results show that in the neuronal phase, the gene expression levels of both MCT8 and MCT10 were increased in RTT cells. This response was probably to increase T4 uptake, since the gene expression levels of DIO2 was greatly reduced in these RTT-derived cells. It is plausible that this was an attempt to compensate for the anticipated deficiency in the hormone that is essential for neuronal function.

Previous studies crossbreeding Dio1/Dio2 knockout mice with Mct8 knockouts resulted in minor neuronal defects, with attenuated gene expression in the neural cortex, an area which is usually upregulated by T3. Aside from these observations, most of the neuronal function and development were normal [21, 38]. Nonetheless, humans with MCT8 deficiencies present abnormal serum TH levels and display severe brain development defects (i.e., psychomotor disorder) [21, 38, 39].

Herein, not only was the *MCT10* gene expression variable at each evaluated phase of cellular differentiation, different

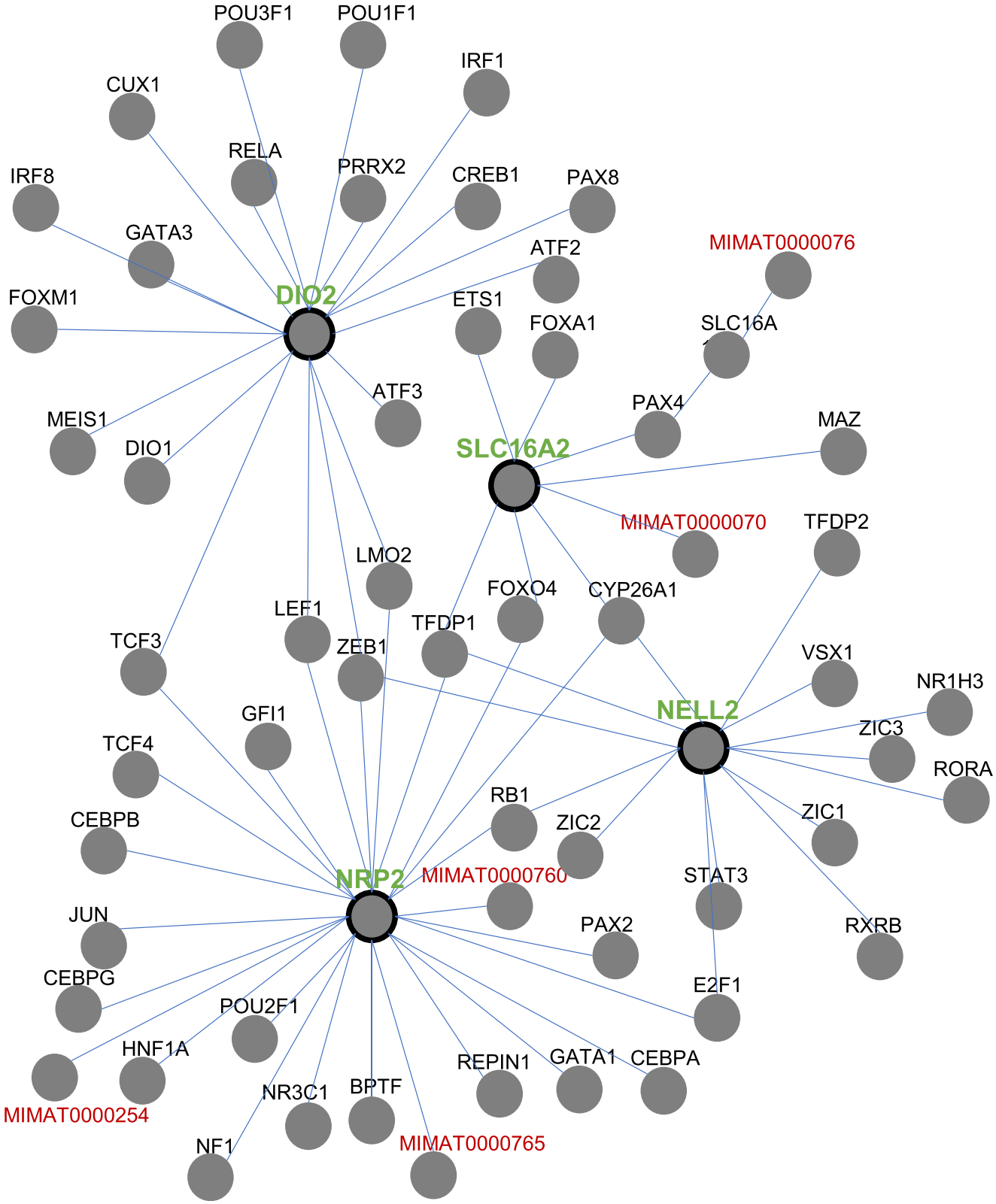

Fig. 6 Metabolic pathways: genetic interaction of affected genes in Rett Syndrome. Genetic interacting network of genes showing altered expression profile in RTT neurons. Interactions were based on experimentally validated databanks [33]

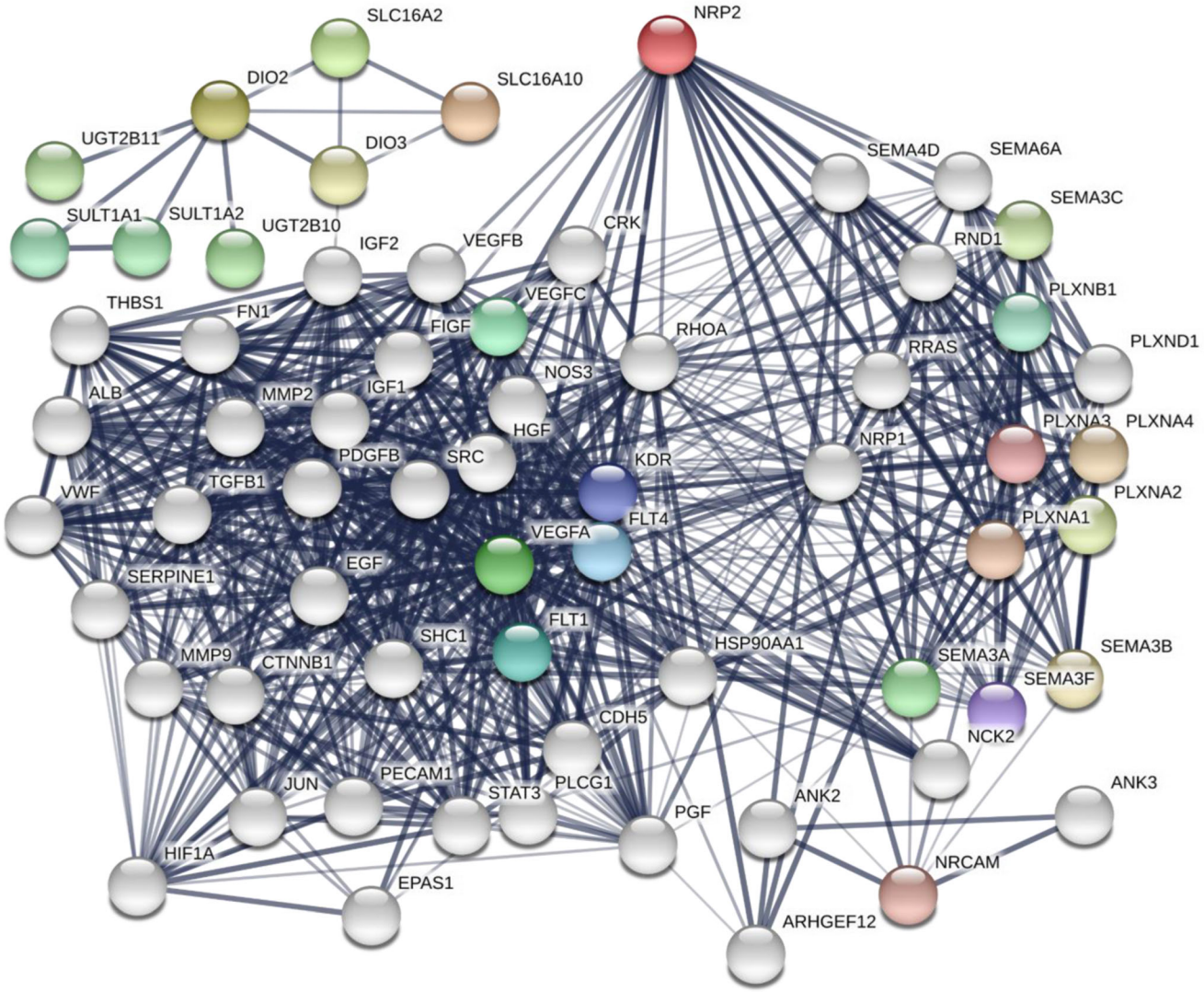

Fig. 7 Metabolic pathways: protein interaction of affected genes in Rett Syndrome. Protein-Protein interaction network of differentially expressed genes in RTT neurons. Network analysis was based on the String software using as input the four protein coding genes showing significant expression alteration in neuronal cells of RTT compared to WT

MCT10 expression levels were detected in RTT cells, when compared to WT. Additionally, the expression levels of *DIO1* in RTT are different when compared to controls in the iPSC phase. This is in contrast to what happens in the EB and NPC stages, where *DIO1* expression in RTT cells is increased when compared to WT.

Interestingly, studies have also shown that the deiodinases in the CNS are differentially expressed. For example, DIO2, typically expressed in astrocytes [31, 40], has been shown to be significantly reduced in RTT neuronal cells compared to WT. It is shown that 80% of T3 present in the brain is produced locally from T4 [41], a process that is dependent on DIO2. Therefore, it is reasonable to assume that the neuronal cells from RTT patients are in a hypothyroid state, since reduced *DIO2* expression has been related to a reduction in the amount of T3 delivered to the brain, thus promoting hypothyroidism [42].

The status of *DIO3* in neural cells is normal and when RTT cells were treated with T3, these cells were capable of increasing the levels of this gene. DIO3 is mainly expressed in neurons and functions to reduce excess T4 levels, generating rT3 and T2, while in astrocytes this enzyme generates T3 from T4 [31, 40]. DIO3 is regulated, at the transcriptional level, by T3 concentrations, mediated by the TRα1 TH receptor [43].

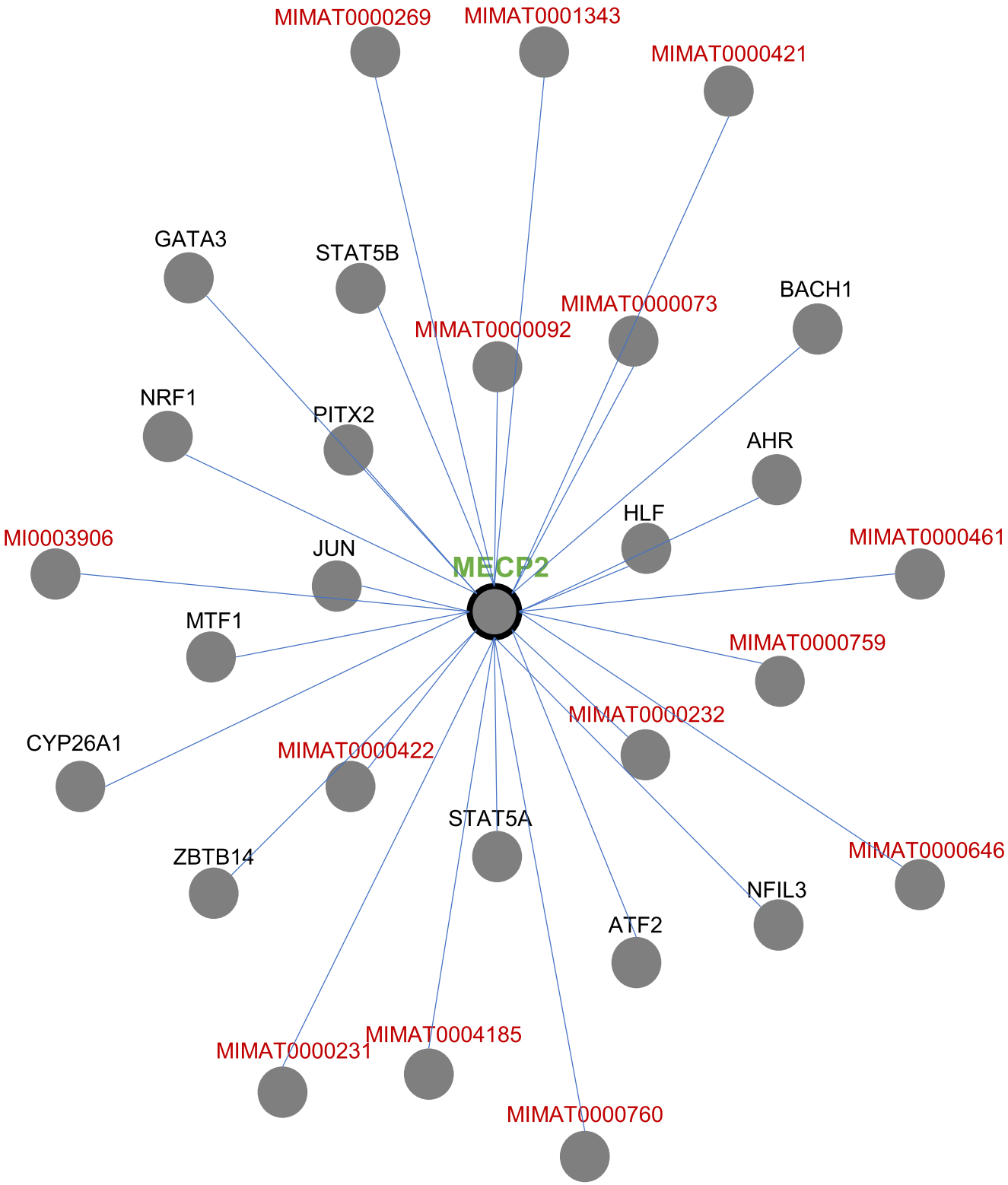

Fig. 8 Metabolic pathways: *MECP2* interaction with possible genes related to neuronal disability. Genetic interaction network of genes directly connected to *MECP2*. Interactions were based on experimentally validated databanks [33]

Here, it was shown that TH treatment increased the levels of synapsin-1 and MAP2 in WT (synapsin-1) and RTT (synapsin-1 and MAP2) in 6 weeks of neuronal cells. This result is in agreement with previous studies that showed that THs promote dendritic and synaptic plasticity [44, 45].

Table 2 Pearson correlation of expressed genes during neuronal phase

r	DIO1	DIO2	DIO3	LAT1	LAT2	MCT8
DIO1	1					
DIO2	0.160	1				
DIO3	0.789***	− 0.111	1			
LAT1	0.633*	− 0.356	0.404	1		
LAT2	0.412	− 0.322	0.637*	0.486	1	
MCT8	0.349	− 0.422	0.476	0.448	0.384	1
MCT10	0.250	− 0.461	0.365	0.477	0.338	*0.959***
OATP4A1	0.391	− 0.192	0.240	0.287	0.576*	0.090
RXRG	0.489	− 0.238	− 0.337	− 0.274	0.125	− 0.201
THRA1	0.619*	− 0.241	0.759**	0.641*	0.666**	0.753**
THRB1	0.533*	− 0.005	0.199	0.713**	0.082	0.152
THRB2	0.551*	− 0.167	0.211	0.602*	− 0.148	0.015
BDNF	0.806***	− 0.006	*0.928***	0.423	0.441	0.370
CYTG	0.183	− 0.291	− 0.033	0.207	0.430	0.138
MAP2	0.652*	− 0.167	*0.927***	0.287	0.477	0.567*
NaKATPase	0.044	− 0.233	0.082	0.261	0.447	0.225
NCAM	− 0.093	− 0.238	0.075	0.203	0.438	0.212
NPR1	*0.860***	− 0.083	0.632*	0.764***	0.265	0.327
NPR2	0.659**	− 0.420	0.724**	0.747**	0.460	0.465
NGB	0.142	− 0.121	0.424	0.144	0.574*	0.162
NGF	0.093	− 0.216	− 0.038	0.309	0.368	0.149
NLGN3	0.325	− 0.391	0.671**	0.213	0.340	0.661**
NLGN4	0.631*	− 0.199	0.757**	0.514	0.456	*0.854***
NRX1	0.552*	− 0.256	*0.853***	0.303	0.443	0.655**
NTF3	0.438	− 0.419	0.119	0.315	0.298	− 0.334
PLXNA1	0.668**	− 0.403	0.781***	0.694**	0.589*	0.415
PLXNB3	0.809***	− 0.151	0.803***	0.337	0.376	0.008
SEMA3A	*0.863***	− 0.038	*0.889***	0.516	0.542*	0.564*
SEMA3C	0.709**	− 0.246	0.536*	0.839***	0.334	0.225
SEMA5A	0.466	− 0.496	0.416	0.745**	0.281	0.470
SHANK3	0.432	− 0.551***	0.588*	0.707 V	0.541*	0.540*
SYN1	0.349	− 0.437	0.696**	0.370	0.618*	0.498
SYT1	− 0.011	− 0.230	0.171	0.231	0.474	0.264
r	MCT10	OATP4A1	RXRG	THRA1	THRB1	THRB2
DIO1						
DIO2						
DIO3						
DIO3						
LAT2						
MCT8						
MCT10	1					
OATP4A1	− 0.052	1				
RXRG	− 0.071	− 0.136	1			
THRA1	0.716**	0.288	− 0.310	1		
THRB1	0.242	− 0.166	− 0.535*	0.348	1	
THRB2	0.091	− 0.174	− 0.583*	0.270	*0.976***	1
BDNF	0.249	0.151	− 0.564*	0.710**	0.365	0.406
CYTG	0.108	0.209	− 0.030	0.221	− 0.008	− 0.078
MAP2	0.439	0.103	− 0.483	0.748***	0.162	0.170

Table 2 (continued)

NaKATPase	0.174	0.230	− 0.121	0.310	0.061	0.000
NCAM	0.158	0.213	− 0.116	0.302	0.012	− 0.046
NPR1	0.336	0.103	− 0.476	0.551*	0.817***	0.795***
NPR2	0.485	− 0.036	− 0.416	0.727**	0.700**	0.642**
NGB	0.055	0.268	− 0.241	0.432	− 0.025	− 0.022
NGF	0.1350	0.171	− 0.092	0.245	0.154	0.088
NLGN3	0.554*	− 0.030	− 0.512	0.674**	0.105	0.063
NLGN4	0.791***	0.157	− 0.507	*0.883***	0.355	0.291
NRX1	0.564*	0.015	− 0.479	0.798***	0.228	0.209
NTF3	− 0.426	0.752**	− 0.311	0.051	0.231	0.296
PLXNA1	0.377	0.752**	− 0.466	0.739**	0.526	0.478
PLXNB3	0.127	0.338	− 0.541	0.440	0.352	0.434
SEMA3A	0.519	0.256	− 0.298	0.803***	0.379	0.376
SEMA3C	0.284	− 0.032	− 0.238	0.513	0.773***	0.735*
SEMA5A	0.550*	− 0.080	− 0.365	0.580*	0.776***	0.673**
SHANK3	0.506	0.167	− 0.483	0.743**	0.476	0.383
SYN1	0.387	0.235	− 0.461	0.713**	0.119	0.074
SYT1	0.197	0.225	− 0.174	0.372	0.043	− 0.011
r	BDNF	CYTG	MAP2	NaKATPase	NCAM	NPR1
DIO1						
DIO2						
DIO3						
LAT1						
LAT2						
LAT2						
MCT10						
OATP4A1						
RXRG						
THRA1						
THRB1						
THRB2						
BDNF	1					
CYTG	− 0.111	1				
MAP2	*0.933***	− 0.073	1			
NaKATPase	0.006	*0.983***	0.033	1		
NCAM	0.000	*0.986***	0.044	*0.996***	1	
NPR1	0.677**	− 0.171	0.518	− 0.063	− 0.117	1
NPR2	0.750**	0.102	0.694**	0.175	0.151	*0.850***
NGB	0.356	0.837***	0.379	*0.874***	*0.890***	0.017
NGF	− 0.087	*0.977***	− 0.099	*0.982***	*0.971***	− 0.056
NLGN3	0.716**	0.080	*0.882***	0.140	0.169	0.296
NLGN4	0.739**	0.010	0.842***	0.120	0.113	0.580*
NRX1	*0.863***	0.007	*0.966***	0.103	0.119	0.506
NTF3	0.150	0.272	− 0.083	0.306	0.273	0.301
PLXNA1	0.825***	0.118	0.769***	0.306	0.161	0.755**
PLXNB3	*0.858***	− 0.097	0.710**	0.001	− 0.010	0.680**
SEMA3A	0.825***	− 0.200	0.792***	− 0.067	− 0.095	0.760**
SEMA3C	0.608*	− 0.122	0.414	− 0.055	− 0.109	*0.881***
SEMA5A	0.439	0.129	0.416	0.169	0.141	0.793***
SHANK3	0.626*	0.346	0.653*	0.375	0.374	0.562*
SYN1	0.701**	0.387	0.802***	0.420	0.446	0.316
SYT1	0.097	*0.967***	0.141	*0.991***	*0.995***	− 0.048
r	NPR2	NGB	NGF	NLGN3	NLGN4	NRX1
DIO1						
DIO2						
DIO3						
DIO3						
LAT2						
MCT8						
MCT10						
OATP4A1						
RXRG						
THRA1						
THRB1						

Table 2 (continued)

THRB2						
BDNF						
CYTG						
MAP2						
NaKATPase						
NCAM						
NPR1						
NPR2	1					
NGB	0.308	1				
NGF	0.154	0.796***	1			
NLGN3	0.613*	0.375	0.020	1		
NLGN4	0.705**	0.261	0.031	0.824***	1	
NRX1	0.737**	0.391	− 0.017	*0.930***	*0.883***	1
NTF3	0.064	0.335	0.318	− 0.298	− 0.124	− 0.171
PLXNA1	*0.937***	0.384	0.117	0.696**	0.713**	0.772***
PLXNB3	0.627*	0.366	− 0.081	0.418	0.432	0.596*
SEMA3A	0.704**	0.162	− 0.146	0.506	0.799***	0.762**
SEMA3C	0.838***	− 0.013	− 0.007	0.219	0.438	0.395
SEMA5A	*0.900***	0.137	0.187	0.462	0.592*	0.532*
SHANK3	*0.851***	0.466	0.336	0.749**	0.716**	0.709**
SYN1	0.679**	0.656*	0.311	*0.882***	0.706**	0.831***
SYT1	0.221	*0.921***	*0.954***	0.244	0.197	0.212
r	NTF3	PLXNA1	PLXNB3	SEMA3A	SEMA3C	SEMA5A
DIO1						
DIO2						
DIO3						
LAT1						
LAT2						
MCT8						
MCT10						
OATP4A1						
RXRG						
THRA1						
THRB1						
THRB2						
BDNF						
CYTG						
MAP2						
NaKATPase						
NCAM						
NPR1						
NPR2						
NGB						
NGF						
NLGN3						
NLGN4						
NRX1						
NTF3	1					
PLXNA1	0.182	1				
PLXNB3	0.506	0.731**	1			
SEMA3A	0.139	0.678**	0.668**	1		
SEMA3C	0.170	0.730**	0.524	0.627*	1	
SEMA5A	0.026	0.797***	0.368	0.496	0.728**	1
SHANK3	0.076	*0.913***	0.472	0.464	0.578*	0.784***
SYN1	0.045	0.824***	0.542*	0.459	0.284	0.509
SYT1	0.279	0.233	0.073	− 0.004	− 0.062	0.185
r	SHANK3	SYN1	SYT1			
DIO1						
DIO2						
DIO3						
LAT1						
LAT2						
MCT8						
MCT10						

Table 2 (continued)

OATP4A1			
RXRG			
THRA1			
THRB1			
THRB2			
BDNF			
CYTG			
MAP2			
NaKATPase			
NCAM			
NPR1			
NPR2			
NGB			
NGF			
NLGN3			
NLGN4			
NRX1			
NTF3			
PLXNA1			
PLXNB3			
SEMA3A			
SEMA3C			
SEMA5A			
SHANK3	1		
SYN1	*0.882***	1	
SYT1	0.426	0.510	1

NTF3 gene expression was used to confirm the effectiveness of T3 treatment [46, 47]. Indeed, when control neuronal cells were treated with T3 (10^{-6} M), the expression of this gene was increased, thus confirming that the TH-responsiveness of the treatment.

The expression of Neuropilin 2 (NPR2), a transmembrane protein, was monitored since this protein has been shown to bind to semaphorins (SEMA). NPR2 is SEMA3F and SEMA3C receptor regulating axon guidance and dendritic patterning. Together with NPR1, NPR2 is important for normal aspects of nervous system development. In fact, disruption in semaphorin signaling can potentially damage axon development [48]. In our study, *NPR2* expression increased in RTT neuronal cells, when compared to controls. There was also a strong correlation identified between the expression of *NPR2*, *SEMAs*, and other SEMA receptors, at the neural stage evaluated.

Monitoring the expression of TH genes that were significantly altered in RTT-derived neurons provide evidence that TH hormones influence and contribute to the RTT phenotype. According to the genetic network presented in Fig. 6, *DIO2* is connected to several genes, some of which are known to be linked to neurological disorders such as involving *CREB1* [49] and *GATA3* [36]. Additionally, the *SLC16A2/MCT8* gene was another important TH gene that presented significantly altered expression when evaluating its expression in RTT compared to WT. This gene genetically interacts with *DIO2*, via the *LEF1* gene, which has been implicated with the normal development of the hippocampus and dentate gyrus [50]. Alterations in *DIO2* expression could compromise normal *TCF3* gene function, which was previously ascribed key roles in the WNT pathway, and is required for the maintenance of normal neuronal stem cell populations during neocortical development [51]. Together, these data suggest that changes in TH expression levels could directly interfere with normal CNS development and function. Interestingly, administering THs to WT and RTT-derived neurons demonstrated that theses hormones modulate synapsin-1 expression, in both groups of cells and MAP2 expression in RTT. Moreover, TH treatment was also capable of rescuing some RTT-associated phenotypes.

As shown in Fig. 9, the hypothetical situation that underlies the TH homeostasis in RTT is presented, and illustrates the expression profiles of the genes affected. It also indicates that throughout all of the cell stages, TH homeostasis is affected to some extent. For example, during the NPC, necessary for neuronal cell differentiation into neuronal cells, and neuronal cell stages, it is likely that a hypothyroid situation is established, since TH levels are reduced. In addition, during the NPC phase, there was an observed decrease *MCT8* gene expression and concomitant increase in *DIO3* expression, a scenario that will effectively inactivate active hormone [52]. At the neuronal cell stage, *DIO2* gene expression was found to be decreased. Thus, even employing other genes, in an attempt to compensate for the lack of active hormone, may prove to be an ineffective mechanism, given the genetic deficiency of the main activator in this process. The results of this study provide important and relevant information regarding the regulatory mechanism(s) related to the impairment of neurodevelopment observed in RTT patients.

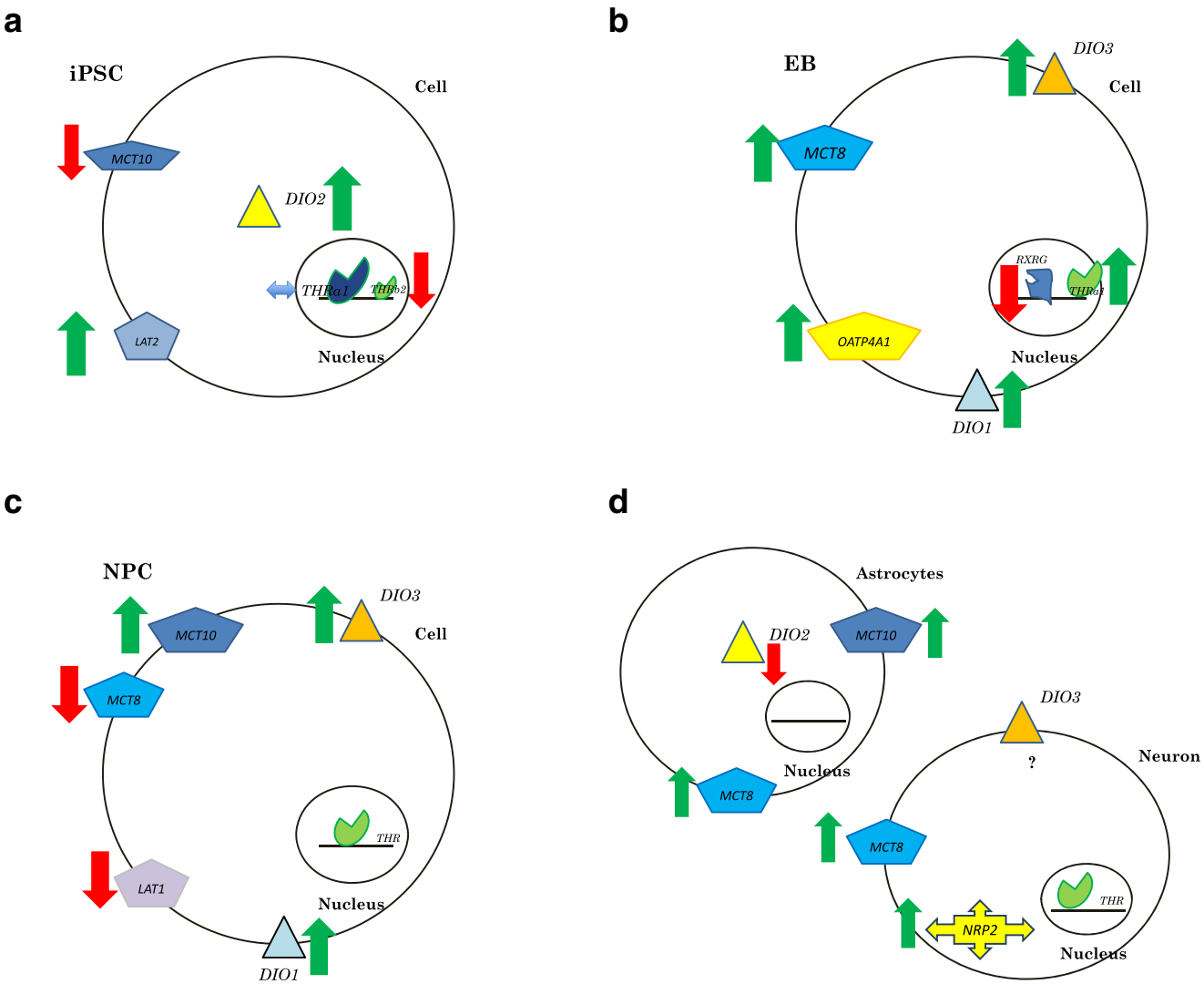

Fig. 9 Hypothetical mechanism involved in cell regulation in each stage of differentiation. Gene expression. **a** iPSC scheme representation of possible TH homeostasis in RTT situation. Affected TH transporters: *MCT10* (decreased), *LAT2* (increased); affected Deiodinase: *DIO2* (increased); affected receptor: *THRB2* (decreased). **b** EB scheme representation of possible TH homeostasis in RTT situation. Affected TH transporters: *MCT8* (increased), *OATP4A1* (increased); affected Deiodinases: *DIO1* (increased), *DIO3* (increased); affected receptor: *THRA1* (increased), *RXRG* (decreased). **c** NPC scheme representation of possible TH homeostasis in RTT situation. Affected TH transporters: *MCT8* (increased), *MCT10* (decreased), *LAT1* (decreased); affected Deiodinases: *DIO1* (increased), *DIO3* (increased). **d** Neural Cells scheme representation of possible TH homeostasis in RTT situation. Affected TH transporters: *MCT8* (increased), *MCT10* (increased); affected Deiodinases: *DIO2* (decreased); affected synapse guidance gene: *NPR2* (increased)

In conclusion, the present study demonstrated that TH homeostasis is compromised in RTT, as evidenced by altered gene expression profiles of deiodinases and transporters. These observations may contribute to the neurodevelopmental characteristics associated with this syndrome.

Acknowledgments This work was supported by a NARSAD Independent Investigator Grant to A.R.M., and the Coordenação de Aperfeiçoamento de Pessoal de Nível Superior (CAPES, Brasilia, Brazil) 18952-12-7 and Fundação de Amparo a Pesquisa do Estado de São Paulo (FAPESP, São Paulo, Brazil) 2017/07053-3 to J.S.S., and from Fundação de Amparo a Pesquisa do Estado de São Paulo (FAPESP, São Paulo, Brazil) 2014/08049-1 to B.H.S.A.

Compliance with Ethical Standards

This study is part of a reviewed and approved research by the UCSD Human Research Protections Program and it is in accordance with requirements of the Code of Federal Regulations on the Protection of Human Subjects (reference number is 090801ZF).

Conflict of Interest Dr. Muotri is a co-founder and has equity interest in TISMOO, a company dedicated to genetic analysis focusing on therapeutic applications customized for autism spectrum disorder and other neurological disorders with genetic origins. The terms of this arrangement have been reviewed and approved by the University of California San Diego in accordance with its conflict of interest policies.

References

1. Hagberg B, Alcardi J, Dias K, Ramos O (1983) A progressive syndrome of autism, dementia, ataxia, and loss of purposeful hand use in girls: Rett's syndrome: report of 35 cases. Ann Neurol 14(4): 471–479
2. Stagi S, Cavalli L, Congiu L, Scusa MF, Ferlini A, Bigoni S, Benincasa A, Rossi B (2015) Thyroid function in Rett syndrome. Horm Res Paediatr 83:118–125
3. Amir RE, Van den Veyver IB, Wan M, Tran CQ, Francke U, Hy Z (1999) Rett syndrome is caused by mutations in X-linked MECP2, encoding methyl-CpG-binding protein 2. Nat Genet 23(2):185–188
4. Marchetto MCN, Carromeu C, Acab A, Yu D, Yeo GW, Mu Y, Chen G, Gage FH et al (2010) A model for neural development and treatment of Rett syndrome using human induced pluripotent stem cell. Cell 143:527–539
5. de Souza JS, Carromeu C, Torres LB, Araujo BHS, Cugola FR, Maciel RMB, Muotri AR, Giannocco G (2017) IGF1 neuronal response in the absence of MECP2 is dependent on TRalpha3. Hum Mol Genet 26(2):270–281
6. Delong GR, Stanbury JB, Fierro-Benitez R (1985) Neurological signs in congenital iodine-deficiency disorder (endemic cretinism). Dev Med Child Neurol 27:317–324
7. Horn S, Heuer H (2010) Thyroid hormone action during brain development: more questions than answers. Mol Cell Endocrinol 315:19–26
8. Chatonnet F, Picou F, Fauquier T, Flamant F (2011) Thyroid hormone action in cerebellum and cerebral cortex development. J Thyroid Res 2011:1–8
9. Ibhazehiebo K, Iwasaki T, Kimura-Kuroda J, Miyazaki W, Shimokawa N, Koibuchi N (2011) Disruption of thyroid hormone receptor-mediated transcription and thyroid hormone-induced Purkinje cell dendrite arborization by polybrominated diphenyl ethers. Environ Health Perspect 119(2):168–175
10. Ibhazehiebo K, Iwasaki T, Okano-Uchida T, Shimokawa N, Ishizaki Y, Koibuchi N (2011) Suppression of thyroid hormone receptor-mediated transcription and disruption of thyroid hormone-induce cerebellar morphogenesis by the polybrominated biphenyl mixture, BP-6. Neurotoxicology 32:400–409
11. Patel J, Landers K, Li H, Mortimer RH, Richard K (2011) Thyroid hormones and fetal neurological development. J Endocrinol 209:1–8
12. de Souza JS, da Conceição RR, Oliveira KC, Maciel RMB, Giannocco G (2016) The hypothyroid brain. Receptors Clin Investig 3(4). https://doi.org/10.14800/rci.1408
13. Berbel P, Obregon MJ, Bernal J, Escobar Del Rey F, De Escobar GM (2007) Iodine supplementation during pregnancy: a public health challenge. Trends Endocrinol Metab 18:338–343
14. Bath SC (2019) The effect of iodine deficiency during pregnancy on child development. Proc Nutr Soc 15:1–11
15. De Escobar GM, Obregón MJ, Del Rey FE (2004) Maternal thyroid hormones early in pregnancy and fetal brain development. Best Pract Res Clin Endocrinol Metab 18(2):225–248
16. Andersen SL (2019) Frequency and outcomes of maternal thyroid function abnormalities in early pregnancy. Scand J Clin Lab Invest 8:1–9
17. Gilbert ME, Rovet J, Chen Z, Koibuchi N (2012) Developmental thyroid hormone disruption: prevalence, environmental contaminants and neurodevelopmental consequences. Neurotoxicology 33(4):842–852
18. Ahmed OM, El-Gareib AW, El-Bakry AM, Abd El-Tawab SM, Ahmed RG (2008) Thyroid hormones states and brain development interactions. Int J Dev Neurosci 26:147–209
19. Manzano J, Bernal J, Morte B (2007) Influence of thyroid hormones on maturation of rat cerebellar astrocytes. Int J Dev Neurosci 25(3):171–179
20. Mendes-de-Aguiar CB, Alchini R, Decker H, Alvarez-Silva M, Tasca CI, Trentin AG (2008) Thyroid hormone increases astrocytic glutamate uptake and protects astrocytes and neurons against glutamate toxicity. J Neurosci Res 86(14):3117–3125
21. Schroeder AC, Privalsky ML (2014) Thyroid hormones, T3 and T4, in the brain. Front Endocrinol 5:1–6
22. Friesema EC, Jansen J, Milici C, Visser TJ (2005) Thyroid hormone transporters. Vitam Horm 70:137–167
23. Chan SY, Martín-Santos A, Loubière LS, González AM, Stieger B, Logan A, McCabe CJ, Frnaklyn JA et al (2011) The expression of thyroid hormone transporters in the human fetal cerebral cortex during early development and in N-Tera-2 neurodifferentiation. J Physiol 589(11):2827–2845
24. Bernal J (2005) The significance of thyroid hormone transporters in the brain. Endocrinology 146(4):1698–1700
25. Heuer H (2011) Hear, hear! Thyroid hormone transporters in cochlear development. Endocrinology 152(12):4478–4480
26. Brent GA, Moore DD, Larsen PR (1991) Thyroid hormone regulation of gene expression. Annu Rev Physiol 53:17–35
27. Lazar MA (1993) Thyroid hormone receptors: multiple forms, multiple possibilities. Endocr Rev 14:184–193
28. Harvey CB, Williams G (2002) Mechanism of thyroid hormone action. Thyroid 12(6):441–446
29. Bernal J (2007) Thyroid hormone receptors in brain development and function. Nat Clin Pract Endocrinol Metab 3:249–259
30. Nageshappa S, Carromeu C, Trujillo CA, Mesci P, Espuny-Camacho I, Pasciuto E, Vanderhaeghen P, Verfaillie CM et al (2016) Altered neural network and rescue in human *MECP2* duplication model. Mol Psychiatry 21(2):178–188
31. Freitas BCG, Gereben B, Castillo M, Kalló I, Zeöld A, Egri P, Liposits Z, Zavacki AM et al (2010) Paracrine signaling by glial cell-derived triiodothyronine activates neuronal gene expression in the rodent brain and human cells. J Clin Invest 120(6):2206–2217
32. Dussault AA, Pouliot M (2006) Rapid and simple comparison of messenger RNA levels using real-time PCR. Biol Proced Online 8(1):1–10
33. Cerami EG, Gross BE, Demir E, Rodchenkov I, Babur O, Anwar N, Schultz N, Bader GD et al (2011) Pathway Commons, a web resource for biological pathway data. Nucleic Acids Res 39(Database issue):D685–D690
34. Szklarczyk D, Franceschini A, Wyder S, Forslund K, Heller D, Huerta-Cepas J, Simonovic M, Roth A et al (2015) STRING v10: protein-protein interaction networks, integrated over the tree of life. Nucleic Acids Res 43(Database issue):D447–D452
35. Hosseinpour M, Mashayekhi F, Bidabadi E, Salehi Z (2017) Neuropilin-2 rs849563 gene variations and susceptibility to autism in Iranian population: a case-control study. Metab Brain Dis 32(5): 1471–1474
36. Wall DP, Esteban FJ, Deluca TF, Huyck M, Monaghan T, Velez de Mendizabal N, Goñí J, Kohane IS (2009) Comparative analysis of neurological disorders focuses genome-wide search for autism genes. Genomics 93(2):120–129
37. Kapoor R, Desouza LA, Nanavaty IN, Kernie SG, Vaidya VA (2012) Thyroid hormone accelerates the differentiation of adult hippocampal progenitors. J Neuroendocrinol 24:1259–1271
38. Braun D, Kinne A, Bräuer AU, Sapin R, Klein MO, Köhrle J, Wirth EK, Schweizer U (2011) Developmental and cell type-specific expression of thyroid hormone transporters in the mouse brain and primary brain cells. Glia 59:463–471
39. Groeneweq S, Visser WE, Visser TJ (2017) Disorder of thyroid hormone transport into tissues. Best Pract Res Clin Endocrinol Metab 31(2):241–253

40. Dentice M, Luongo C, Huang S, Ambrosio R, Elefante A, Mirebeau-Prunier D, Zavacki AM, Fenzi G et al (2007) Sonic hedgehog-induced type 3 deiodinase blocks thyroid hormone action enhancing proliferation of normal and malignant keratinocytes. Proc Natl Acad U S A 104(36):14466–14471
41. Crantz FR, Silva JE, Larsen PR (1982) An analysis of the sources and quantity of 3,5,3′-triiodothyronine specifically bound to nuclear receptors in rat cerebral cortex and cerebellum. Endocrinology 110(2):367–375
42. Galton VA, Wood ET, St Germain EA, Withrow CA, Aldrich G, St Germain GM, Clark AS, St Germain DL (2007) Thyroid hormone homeostasis and action in type 2 deiodinase-deficient rodent brain during development. Endocrinology 148(7):3080–3088
43. Gil-Ibáñez P, Bernal J, Morte B (2014) Thyroid hormone regulation of gene expression in primary cerebrocortical cells: role of thyroid hormone receptor subtypes and interactions with retinoic acid and glucocorticoids. PLoS One 9(3):e91692
44. Min H, Dong J, Wang Y, Wang Y, Teng W, Xi Q, Chen J (2016) Maternal hypothyroxinemia-induced neurodevelopmental impairments in the progeny. Mol Neurobiol 53(3):1613–1624
45. Boukhtouche F, Brugg B, Wehrlé R, Bois-Joyeux B, Danan JL, Dusart I, Mariani J (2010) Induction of early Purkinje cell dendritic differentiation by thyroid hormone requires RORa. Neural Dev 5:18
46. Fauquier T, Romero E, Picou F, Chatonnet F, Nguyen XN, Quignodon L, Flamant F (2011) Severe impairment of cerebellum development in mice expressing a dominant-negative mutation inactivating thyroid hormone receptor alpha1 isoform. Dev Biol 356(2):350–358
47. Grijota-Martínez C, Samarut E, Scanian TS, Morte B, Bernal J (2011) In vivo activity of the thyroid hormone receptor beta- and α-selective agonists GC-24 and CO23 on rat liver, heart and brain. Endocrinology 152(3):1136–1142
48. Raimondi C, Ruhrberg C (2013) Neuropilin signaling in vessels, neurons and tumours. Semin Cell Dev Biol 24(3):172–178
49. Jang DH, Chae H, Kim M (2015) Autistic and Rett-like features associated with 2q33.3-q34 interstitial deletion. Am J Med Genet A 167A(9):2213–2218
50. Galceran J, Miyashita-Lin EM, Devaney E, Rubinstein JL, Grosschedl R (2000) Hippocampus development and generation of dentate gyrus granule cells is regulated by LEF1. Development 127:469–482
51. Kuwahara A, Sakai H, Xu Y, Itoh Y, Hirabayashi Y, Gotoh Y (2014) Tcf3 represses Wnt-β-catenin signaling and maintains neural stem cell population during neocortical development. PLoS One 9(5):e94408
52. Baqui M, Botero D, Gereben B, Curcico C, Harney JW, Salvatore D, Sorimachi K, Larsen PR et al (2003) Human type 3 iodothyronine selenodeiodinase is located in the plasma membrane and undergoes rapid internalization to endosomes. J Biol Chem 278(2):1206–1211